

Chapter III.3

Introduction to CERN and its accelerator complex

Reyes Alemany Fernández

CERN, Geneva, Switzerland

The CERN accelerator complex has evolved over nearly 70 years, from the first 16 m circumference machine in 1957, the Synchrocyclotron, to the most powerful synchrotron in the world to today, the LHC, with 27 km circumference. In between, a series of machines were designed, installed and commissioned and most of them are still in operation serving, with an impressive zoo of particles, the very rich and diverse physics programmes carried out at CERN. This chapter gives an overview of the proton and ion accelerator complex, as well as a summary of the different fixed-target experimental areas and facilities served by the complex.

The CERN Accelerator Complex was born in 1957, three years after CERN foundation, when a 600 MeV, 15.7 m circumference synchrocyclotron, Fig. III.3.1, was installed in Meyrin site. Sixty-seven years later, at the time of writing this book, the CERN Accelerator Complex has more than 70 km of accelerators, including the transfer lines. Some of the machines have already been decommissioned, like the synchrocyclotron after 33 years of service, new ones were built in between, like the Large Hadron Collider (LHC) that started operation in 2008. The oldest, still functional, machine at CERN is the Proton Synchrotron (PS) commissioned in 1959. The youngest ones are ELENA (Extra Low Energy Antiproton ring) and Linac4, both started commissioning in 2020. Figure III.3.2 shows a schematics of the accelerator complex, with all the linacs, synchrotrons, transfer lines and experimental facilities. The zoo of particles that are operated in the current complex, goes from the lightest ones: electrons, protons and H^- ions, to a long list of medium and high mass ions like oxygen, argon, xenon and lead.

This chapter will give some hints of the CERN Accelerator Complex history, before focusing on the present layout and parameters per machine. In particular, it will highlight the most important aspects of the injectors post Long-Shutdown 2 (post-LS2) era, because they underwent an impressive amount of upgrades in order to meet the High-Luminosity LHC (HL-LHC) performance request, i.e. an increase by a factor 2 of the LHC proton-proton collisions integrated luminosity after 10 years of operation to reach 3000 fb^{-1} by 2035, a goal out of reach for the pre-LS2 complex [1]. To achieve this target luminosity, the intensity of the proton beam has to be doubled, and its brightness multiplied by 2.5 ($2.3 \cdot 10^{11}$ protons per bunch with 25 ns bunch spacing within transverse normalized emittances of $2.1 \mu\text{m rad}$). On top of this, the HL-LHC is requested to deliver an integrated luminosity of 10 nb^{-1} of lead-lead collisions at top energy to each of the ALICE, ATLAS and CMS experiments. Achieving this goal requires about a factor 2 higher total intensity from the injectors than what they can produce today.

This chapter should be cited as: Introduction to CERN and its accelerator complex, R. Alemany Fernández, DOI: [10.23730/CYRSP-2024-003.1903](https://doi.org/10.23730/CYRSP-2024-003.1903), in: Proceedings of the Joint Universities Accelerator School (JUAS): Courses and exercises, E. Métral (ed.),

CERN Yellow Reports: School Proceedings, CERN-2024-003, DOI: [10.23730/CYRSP-2024-003](https://doi.org/10.23730/CYRSP-2024-003), p. 1903.

© CERN, 2024. Published by CERN under the [Creative Commons Attribution 4.0 license](https://creativecommons.org/licenses/by/4.0/).

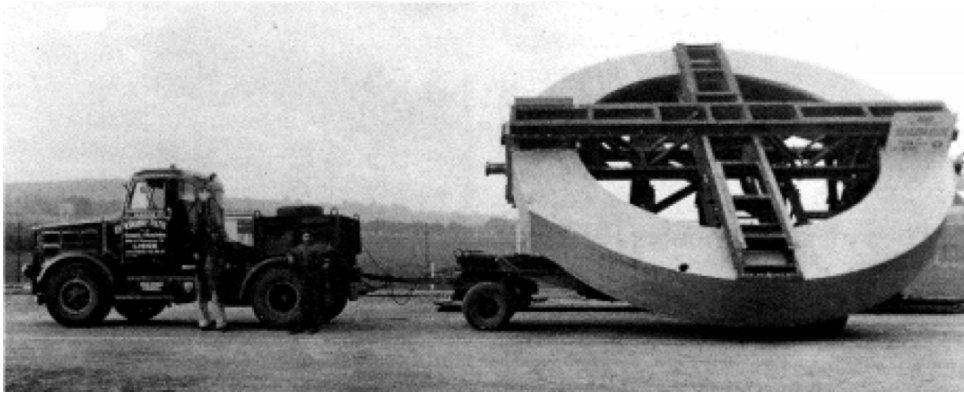


Fig. III.3.1: Magnet core of the Synchrocyclotron, the very first CERN accelerator, being transported to the CERN Meyrin site in 1957.

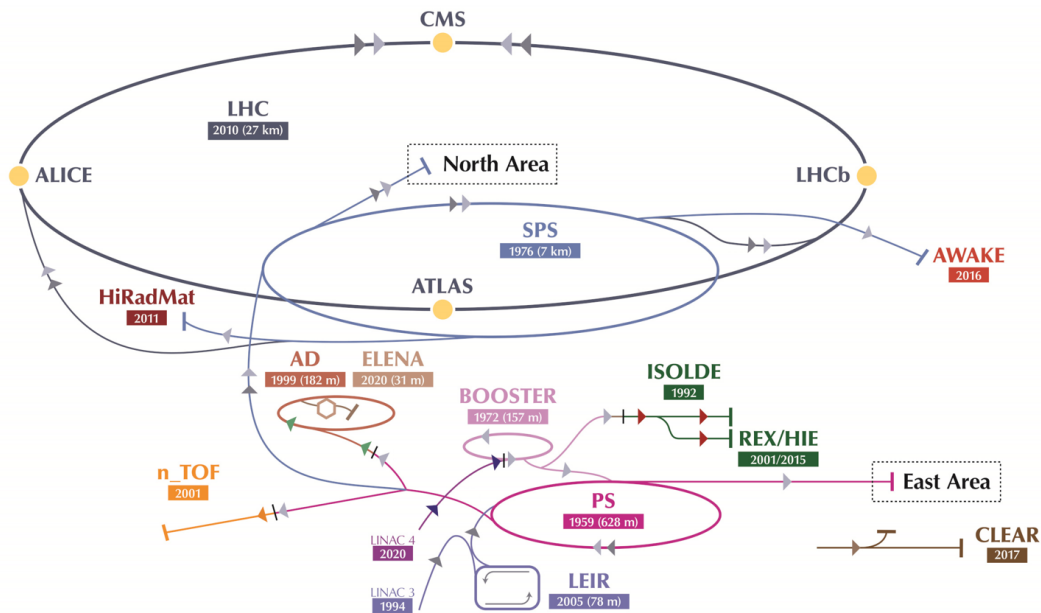


Fig. III.3.2: CERN Accelerator Complex in 2023.

III.3.1 Proton injectors

One of the available parameters to increment the LHC luminosity is to increase the ratio between the bunch intensity and the bunch emittance, i.e. the bunch brightness. The bunch brightness is determined by the injectors, and it is, generally, limited by the space charge generated directly by the charge distribution. Space charge is actually a particular case of Coulomb interactions in a multi-particle system and more severe at low energies. Because the Coulomb interaction happens between charged particles of the same sign, it is a strong repulsive force that modifies the overall focusing field experienced by the beam, and consequently, changes the betatron tune of each particle. If the change of betatron tune is large, the beam can be forced to cross unwanted resonances giving rise to transverse emittance blow-up and eventually beam intensity losses when the bunch transverse dimensions reach the machine aperture. The negative effects of this Coulomb interaction can be very effectively counteracted by increasing the beam energy

because the change in tune is inversely proportional to the relativistic $\beta\gamma^2$ factor. With the pre-LS2 linear accelerator, Linac 2, an increase of the beam energy beyond 50 MeV was not possible, and therefore, a new linac took over the job, Linac4, capable of accelerating particles up to 160 MeV. Moreover, Linac4 was designed for the acceleration of H^- ions instead of protons, to benefit from the advantages of charge-exchange injection into the next synchrotron, the PS Booster, using a stripping foil, a technique already in use in the major accelerator laboratories but never applied at CERN. Charge exchange injection in the Booster will replace multi-turn betatron stacking, increasing the efficiency up to 98% and providing the means to tailor the transverse distribution of protons.

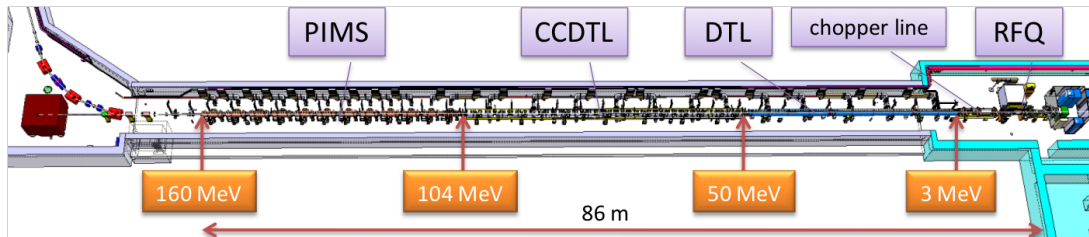


Fig. III.3.3: Linac4 layout. The H^- source is on the right of the RFQ, the beam is accelerated from right to left. The energy increase achieved by the different accelerating structures is indicated in the figure.

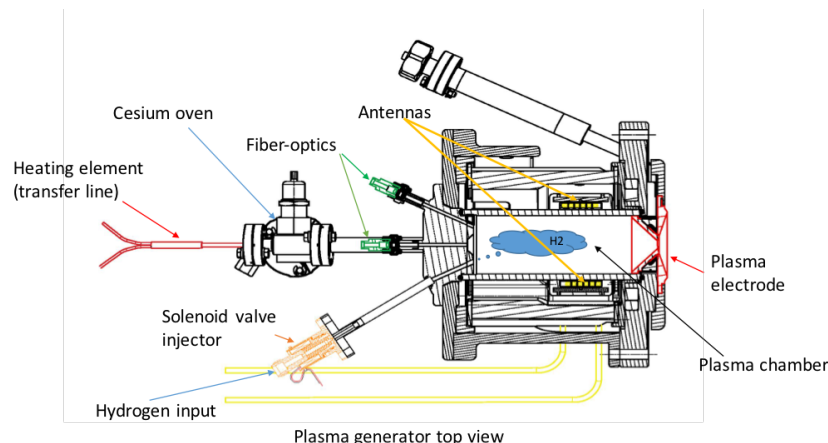


Fig. III.3.4: Linac4 H^- source layout.

Because of the new injection parameters, the Booster had to be upgraded to be able to cope with H^- injection and the new injection energy, 160 MeV. The Booster pre-LS2 injection energy was, of course, 50 MeV. Moreover, the Booster flat-top energy was upgraded from 1.4 to 2 GeV to help mitigating space charge issues in PS, also a bottle-neck for the LHC beams brightness increase. Consequently, the new Booster extraction energy implied the upgrade of the PS injection energy to 2 GeV.

In the SPS pre-LS2, the maximum intensity was limited to $1.2 \cdot 10^{11}$ protons per bunch, because of the available RF power and because of longitudinal coupled-bunch instabilities. Therefore, the SPS upgrade consisted of two new 1.6 MW RF power plants installed to double the available power at 200 MHz, the main accelerating harmonic, and the cavities were reorganized into six assemblies (previously four),

reducing the beam impedance.

III.3.1.1 Linac4

Linac4 [2] consists of an H^- source and a series of accelerating structures, as can be seen in Fig. III.3.3.

The H^- source consists of an hydrogen injection mechanism in a plasma chamber which role is to produce H^- , as sketched in Fig. III.3.4. There are two H^- production mechanisms:

- H^- from the plasma cell via the process: $e + H_2 \rightarrow H^- + H$;
- H^- from the surface via electron transfer from the surface to an atom leaving the surface. This process is enhanced by lowering the surface work function via the deposition of an alkali, e.g. caesium.

The ion source is followed by a low-energy beam transport section that prepares the beam for injection into the RFQ accelerator. The chopper line has a fast deflector, which eliminates individual bunches or trains of bunches on a beam dump. This process is needed because the Booster required bunch length is 650 ns for 1 MHz RF frequency at capture, while the bunches from Linac4 correspond to 352 MHz, therefore only 65% of the Linac4 bunches are injected into the Booster RF bucket. Acceleration is provided by three sections, the first two being equipped with drift tube linac (DTL Fig. III.3.5) structures, the first of a conventional Alvarez type, and the second with a new design with external coupling cells connecting short DTL sections called the cell-coupled drift tube linac (CCDTL Fig. III.3.6). In the third section, a sequence of Pi-mode structure (PIMS Fig. III.3.7) cavities accelerates the beam to the final energy. All the accelerating structures operate at 352.2 MHz frequency; their RF designs allow for a conventional FODO beam optics, required to minimize emittance growth in the linac. The overall length of Linac4, from the ion source to the end of the last PIMS, is 76.33 m. Table III.3.1 compiles the main Linac4 parameters.



Fig. III.3.5: Linac4 DTL layout.

III.3.1.2 Booster

The Booster is a synchrotron with four vertically stacked rings (to mitigate space charge), each 1/4 of PS circumference, Fig. III.3.8-top-left. It has a circumference of 157 m and started operation in 1972.

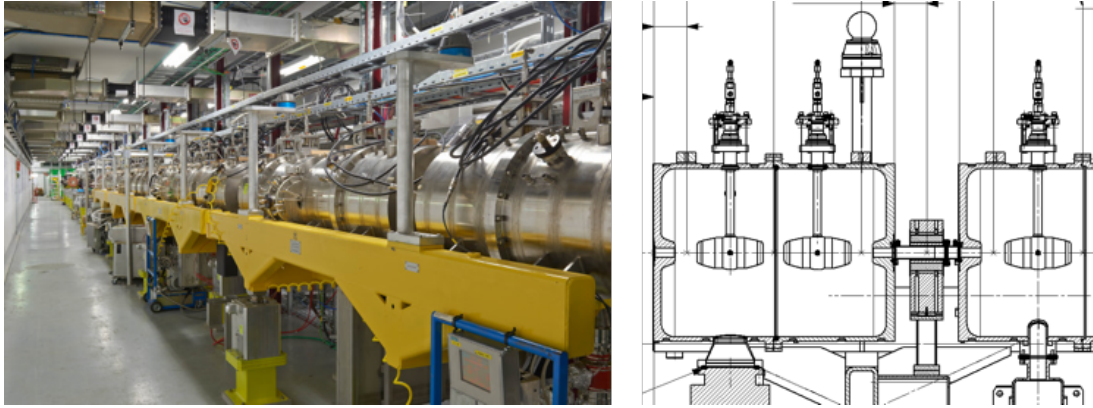


Fig. III.3.6: Linac4 CCDTL layout.



Fig. III.3.7: Linac4 DTL layout.

It was designed and constructed to increase the injection energy in the PS and therefore lift up the beam intensity limitation in PS as requested by the Intersecting Storage Rings (ISR), the world's first hadron collider commissioned on 27 January 1971 at CERN. Its duty cycle is 1.2 s; two cycles are needed to fill the PS with protons for LHC. A detail of the four vertically stacked main dipole magnets can be seen in Fig. III.3.8-top-right.

The upgrade of the Booster [3] during LS2 consisted of a new injection system to accept H^- instead of protons, at a new energy, 160 MeV, and the capability of accelerating the beam to 2 GeV.

With the increase of injection beam energy from 50 to 160 MeV the relativistic $\beta\gamma^2$ factor increases by a factor of 2, thus doubling the intensity that can be accumulated within a given emittance, resulting in a factor 2 brightness increase at Booster injection. This upgrade mainly benefits the ISOLDE beams. The combination of the 160 MeV injection energy and 2 GeV acceleration is what really benefits the LHC beams, together with the H^- injection. The pre-LS2 multi-turn injection of protons, had an intrinsic 50% intensity loss, the new scheme is essentially loss-free (apart from a few percent loss due to stripping efficiency). Figure III.3.8-bottom-left shows the new injection system, one per ring, and

Table III.3.1: Main Linac4 parameters.

Parameter	Value
Ion species	H^-
Output energy	160 MeV
Bunch frequency	352.2 MHz
Maximum repetition rate	2 Hz
Beam pulse length	400 μs
Mean pulse current	40 mA
Maximum number of particles per pulse	$1.0 \cdot 10^{14}$
Number of particles per bunch	$1.14 \cdot 10^9$
Transverse emittance	$0.4 \pi \mu m$ (rms)

Fig. III.3.8-bottom-right shows one of the stripping foils. On the other hand, increasing the flat top energy from 1.4 to 2 GeV brings a gain in space charge tune shift of 1.63, which corresponds to an intensity increase of 60% for a same emittance value.

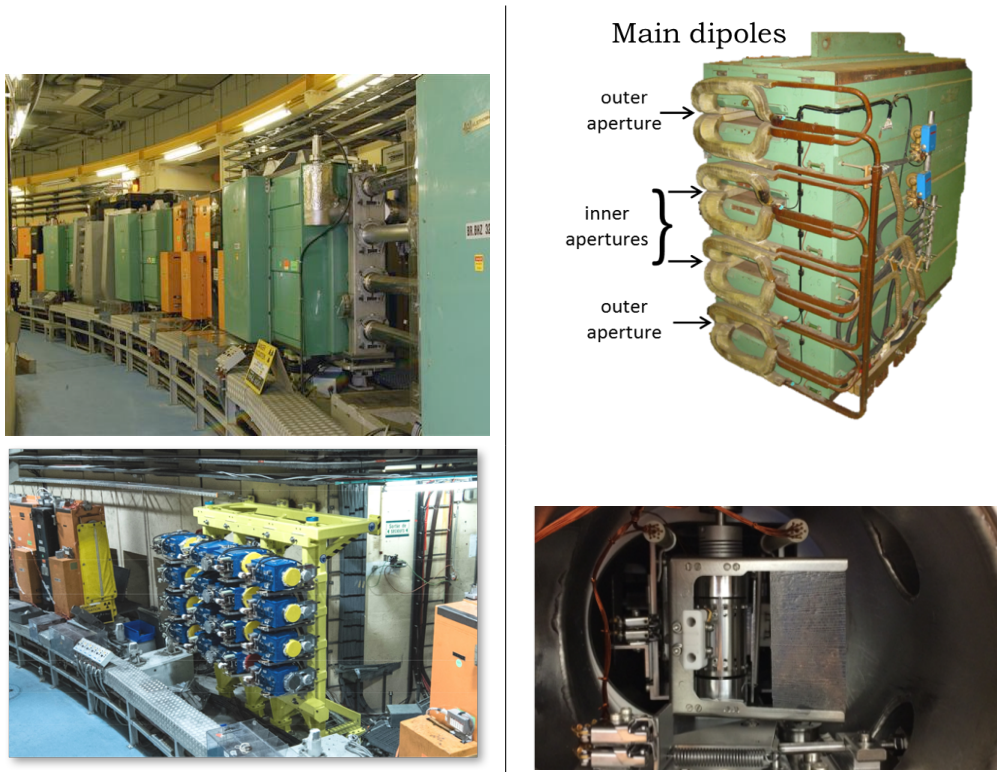


Fig. III.3.8: Top-left: A view of the Booster; top-right: detail of the four vertically stacked main dipole magnets; bottom-left: the new injection system, one per ring; bottom-right: stripping foil.

Besides the already mentioned Booster upgrades during LS2, several others took place as well, some are mentioned below, but the complete list can be found in Ref. [3]:

- Replacement of some RF cavity system by new wide-band cavities;
- Full renovation of the Low-Level RF (LLRF), since the old system was obsolete and inappropriate for Linac4 and new High-Level RF;

- Improved instrumentation for measurement of high brightness beams and for 160 MeV H^- injection;
- New beam dump system.

Table III.3.2 compares the achieved parameters with the pre-LS2 machine with the HL-LHC request for the production of the LHC 25 ns beam.

Table III.3.2: Beam characteristics at Booster injection. N is number of protons per bunch. $\epsilon_{x,y}$ and ϵ_s are the transverse and longitudinal normalized emittances. B_l is the bunch length.

	N (10^{11} p)	$\epsilon_{x,y}$ (μm)	E (MeV)	ϵ_s (eVs)	B_l (ns)
Pre-LS2 (25 ns)	17.73	2.14	50	1.0	1100
HL-LHC (25 ns)	34.21	1.72	160	1.4	650

III.3.1.3 Proton Synchrotron

The Proton Synchrotron (PS), the first alternating gradient machine in the world, with a circumference of 628.32 m, started operation in 1959 and following regular maintenance periods and the upgrade during LS2, is still in operation. For many years it sustained an important program of fixed-target physics and it has provided several types of particles: protons, anti-protons, deuterons, α , oxygen, sulphur, indium, lead, electrons and positrons) to ISR, SPS, the Large Electron Positron collider (LEP) and ISOLDE, until it became a crucial LHC injector. It defines the bunch train structure for all users, including the LHC. It has combined function magnets, i.e. they work as dipoles and quadrupoles at the same time. In many of the synchrotrons constructed later, the bending and the focusing functions are separated (the advantages being a higher bending field and therefore a higher energy for a given circumference, and more flexibility of changing the working point, i.e. the tune), but at that time it was thought natural to incorporate the focusing into the main bending magnets. The upgrade of the PS [3] during LS2 consisted of a new

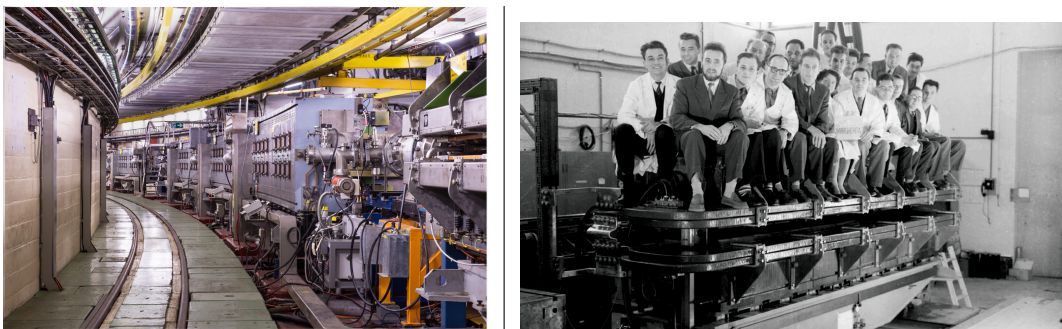


Fig. III.3.9: Left: view of a PS section; right: the first magnet unit produced was called Margherita, from the name of the only woman in the group at that time.

injection system to accept protons at a new energy of 2 GeV, together with new orbit correctors and lattice quadrupoles used at low energy to cope with the new energy. Some other upgrades are mentioned below, but the complete list can be found in Ref. [3]:

- Upgrade of the transverse and longitudinal damper;

- Upgrade of the LLRF to fully digital;
- New 1-turn delay feedback, coupled-bunch feedback and beam loading compensation for the RF cavities;
- New beam dump system.

Table III.3.3 compares the achieved parameters with the pre-LS2 machine with the HL-LHC request for the production of the LHC 25 ns beam.

Table III.3.3: Beam characteristics at PS injection. N is number of protons per bunch. $\epsilon_{x,y}$ and ϵ_s are the transverse and longitudinal normalized emittances. B_l is the bunch length.

	N (10^{11} p)	$\epsilon_{x,y}$ (μm)	E (GeV)	ϵ_s (eVs)	B_l (ns)
Pre-LS2 (25 ns)	16.84	2.25	1.4	1.2	180
HL-LHC (25 ns)	32.50	1.80	2.0	3.0	205

III.3.1.4 Super Proton Synchrotron

The Super Proton Synchrotron (SPS) was born because in the seventies the fixed-target experiments requested higher energies than what the PS could deliver. The SPS is a synchrotron of 6911.5 m circumference, and the first machine built underground. It was commissioned in 1976 to an energy of 300 GeV first, and soon after to 400 GeV. Thanks to the careful design, the top energy could later be increased to 450 GeV at the request of particular experiments and today the SPS accelerates indeed the LHC beams to 450 GeV. It got the first 2 T accelerator magnets produced in history, and the most advanced extraction elements at the time. During its commissioning as a fixed-target accelerator, Carlo Rubbia proposed to convert the SPS into a proton anti-proton collider, Sp \bar{p} S, making use of the stochastic cooling method invented by Simon van der Meer a few years before and tested in the ISR. The idea required the construction of the Anti-Proton Accumulator. The luminosity at the beginning (few 10^{29} $\text{cm}^{-2} \text{s}^{-1}$) was sufficient to allow, relatively quickly, the discovery of the W^\pm and Z electro-weak bosons in 1983.

The upgrade of SPS during the LS2 covered two main domains. On one side a complete refurbishment of the power RF system with the addition of two 1.4 MW power plants, and a new LLRF system based on the state of the art electronics technology. On the other, many of the beam intercepting devices (new beam dump system, collimators upgrade) had to be upgraded to cope with the HL-LHC high intensity beams. Beam diagnostics, power converters and injection systems were also upgraded. The complete list of systems can be found in [3].

Table III.3.4 compares the achieved parameters with the pre-LS2 machine with the HL-LHC request for the production of the LHC 25 ns beam with 4 injections of 36 or 72 bunches.

Table III.3.4: Beam characteristics at SPS injection. N is number of protons per bunch. $\epsilon_{x,y}$ and ϵ_s are the transverse and longitudinal normalized emittances. B_l is the bunch length.

	N (10^{11} p)	$\epsilon_{x,y}$ (μm)	p (GeV/c)	ϵ_s (eVs)	B_l (ns)
Pre-LS2 (25 ns)	1.33	2.36	26	0.42	3.0
HL-LHC (25 ns)	2.57	1.89	26	0.42	3.0



Fig. III.3.10: Top-left: A view of the SPS with main dipole magnets in red and main quadrupole magnets in blue; top-right: the new beam dump system located at Point 5; bottom-left: extraction septa system; bottom-right: travelling wave RF cavities.

III.3.2 Ion injectors

The CERN PS Ion Injector complex consists of an Electron Cyclotron Resonance (ECR) source, a linear accelerator called Linac 3 and the Low Energy Ion Ring (LEIR). The complex transforms low-intensity lead-ion pulses from the source and Linac 3 in high intensity ion bunches via accumulation and beam cooling in LEIR. The PS Ion Injector complex is, together with the PS and SPS, part of the LHC Ion Injector Complex (LIIC), which owes part of its characteristics to the CERN Heavy-Ion Facility built in the 90's to serve the SPS North Area Experiments. From conceptual design to today, the LIIC underwent several upgrades to meet and surpass the LHC luminosity performance originally required, $10^{27} \text{ cm}^{-2}\text{s}^{-1}$, and later by the High-Luminosity LHC era, $7 \cdot 10^{27} \text{ cm}^{-2}\text{s}^{-1}$.

In the context of the LHC Injector Upgrade project [4], an intense program of machine development studies, equipment upgrade and consolidation were launched in the PS Ion Injector complex during Run 2 (2015–2018). The aim being to understand and overcome the intensity limitations that were restricting the extracted lead beam intensity from LEIR to values almost a factor two below the required LIU target of $9 \cdot 10^{10}$ charges extracted. After some brief historical notes, the following sections review the upgrades and the current performance of the ion complex.

III.3.2.1 History of ions at CERN

In the early days of CERN, protons were the only particle type accelerated in the complex. Only in 1964 deuterons were successfully accelerated in the first CERN Linac (often referred to as Linac 1) encouraging the ISR user community to request the first deuterons and later on alpha particles. Without

major difficulties, Linac 1 and the downstream machines demonstrated their capability of accelerating fully stripped ions up to calcium. This success triggered a study at the beginning of the 80's to accelerate heavier ions (oxygen and sulphur). A new ECR source and RFQ, together with a 33% increase of the Linac 1 RF accelerating and focusing fields, were the focus of the first upgrade, followed by the installation, late 80's, of a new 14 GHz Geller source to increase the delivered intensity.

With the field increased by 33%, Linac 1 was at the technological limit of its possibilities. Increasing the beam intensity required a complete renovation of Linac 1. On March 9, 1990, a collaboration between different laboratories and CERN to build the first CERN Heavy-Ion Facility was launched, the Lead-Ion Accelerating Facility, to serve the fixed-target experiment community. The first Heavy-Ion Facility proposal [5, 6] had an ECR-ion source, a low-energy beam transport line with an RFQ, an Interdigital-H linear accelerator, Linac 3, a debuncher and a stripper foil to strip the $^{208}\text{Pb}^{28+}$ (selected after the source) to $^{208}\text{Pb}^{53+}$. The first physics run with the new facility started already in 1994 [7].

The layout described above was, however, unable to satisfy the LHC luminosity requirements by three orders of magnitude. A factor 30 increase in number of ions per bunch was needed, either by increasing the Linac 3 current or by applying storage and cooling techniques, or a combination of both. Therefore, in parallel to the operation of the CERN Heavy-Ion Facility, a study was launched to upgrade the complex to cope with the LHC requirements.

In December 1993, the first LHC ion programme was proposed to the CERN Council as part of the Large Hadron Collider, LHC Project Proposal. Three years later, the LHC Conceptual Design Report [8] was published. In 2000, however, some of the basic input parameters were modified triggering a complete LHC ion programme review [9]. Since 1993 several schemes were considered to fulfil the LHC requirements. Finally the one selected used the conversion *in situ* of the existing Low-Energy Antiproton Ring (LEAR) [10, 11] into a Low-Energy Accumulator Ring, to complete the LHC Ion Complex under the name Low-Energy Ion Ring (LEIR). The final LEIR design appeared in 2003 [12] and in 2004 it was presented as part of the LHC Design Report [1].

Following the initial design and the first operational run, Run 1 (2010-2013), the luminosity required by the High-Luminosity LHC experiments demanded a considerable performance increase of the ion complex. During Run 2 (2015-2018), several improvements were made to be able to meet the bunch intensities and emittances for the fully stripped lead ions at LHC injection, as required by the HL-LHC upgrade (see Table 2.8 in Ref. [13]). The total ion beam intensity at LHC injection required by HL-LHC was only achieved during Run 3 when the SPS slip-stacking mechanism, allowing to reduce the bunch spacing from 100 to 50 ns, was commissioned. During Run 1, Run 2 and Run 3 different ion species were operated in the CERN Ion Accelerator Complex. The ones used for fixed-target or LHC physics are summarised in Table III.3.5. On top of this, the complex carried out tests with other ions.

In the following a description of source, Linac 3 and the LEIR machine, is presented together with the beam performance achieved over the past years.

III.3.2.2 Ion source and Linac 3

The present ion source is called GTS-LHC, Grenoble Test Source (GTS) developed at CEA (France) for the LHC, and is an Electron Cyclotron Resonance Ion Source (ECRIS) [14]. It was installed and

Table III.3.5: List of the different ions species in the accelerator complex during Run 1, Run 2 and Run 3. Pb, Xe and O indicates the fully stripped ions, $^{208}\text{Pb}^{82+}$, $^{129}\text{Xe}^{54+}$ and $^{16}\text{O}^{8+}$, respectively. When the ion is partially stripped the charge is explicitly given. PbPb, pPb, XeXe, pO and OO indicate collisions in LHC. Only the last machine or facility that received the beam is indicated.

	Year	Linac 3	PS	SPS	NA61/SHINE	LHC
Run 1	2010					PbPb
	2011					PbPb , pPb
	2012				Pb	pPb
	2013					pPb
	2014				Pb	
Run 2	2015				Ar	PbPb
	2016				Pb	PbPb
	2017			Xe^{39+}	Xe	XeXe
	2018			Pb^{80+} , Pb^{81+}	Pb	PbPb, Pb^{81+}
Run 3	2022				Pb	PbPb
	2023	Kr^{22+}	O^{4+}		Pb	PbPb
	2024		Mg^{7+}		Pb	PbPb
	2025				Pb, O	PbPb, OO, pO

commissioned in 2005 [15]. The source runs in the afterglow mode. For this the microwave is pulsed at 10 Hz resulting in \sim ms long ion beam pulses. But only \sim 200 μ s of the pulse length is accelerated and not all pulses are sent to LEIR. The source is equipped with gas injection and two independent micro ovens. The extracted beam kinetic energy is 2.5 keV/nucleon (adapted to the RFQ).

The linear accelerator Linac 3 is operational since 1994 [5], accelerating heavy ions from 2.5 keV/nucleon to 4.2 MeV/nucleon for injection and accumulation into LEIR.

Charge state selection is first carried out on the beam extracted from the source via a 135° spectrometer bend, with 0.15 T maximum dipole field. The nominal charge state, 29+ for lead, is filtered and subsequently matched to the first accelerating system by means of a quadrupole triplet and a solenoid. This first stage is called Low-Energy Beam Transport (LEBT) line. Acceleration is then done in two stages. First a 101.28 MHz, 2.5 m long 4-rod Radio-Frequency Quadrupole (RFQ) increases the beam energy to 250 keV/nucleon. The RFQ has been designed in particular to minimize the output beam longitudinal emittance. The Medium-Energy Beam Transport (MEBT) line is composed of two quadrupole doublets and one bunching cavity. Finally, a system of 3 Interdigital-H (IH) tanks (the first one at 101.28 MHz, the other two at 202.56 MHz) takes the beam to 4.2 MeV/nucleon. Between each section, a quadrupole triplet focuses the beam. The beam is then stripped while passing through an amorphous carbon foil, and a new charge state is selected for injection in LEIR. The Linac 3 layout can be found in Fig. III.3.11. The linac can deliver 200 μ s long beam pulses, with a maximum repetition rate of 5 Hz (a burst mode at 100 ms is possible that cannot exceed 5 Hz when averaged).

III.3.2.3 LEIR

The LEIR machine transforms a series of long (\sim 200 μ s), low intensity ion pulses from Linac 3 into high density, short (\sim 200 ns) bunches by accumulation and phase space cooling. Accumulation is achieved by the technique of multi-turn injection. Phase space cooling is achieved by the technique of electron

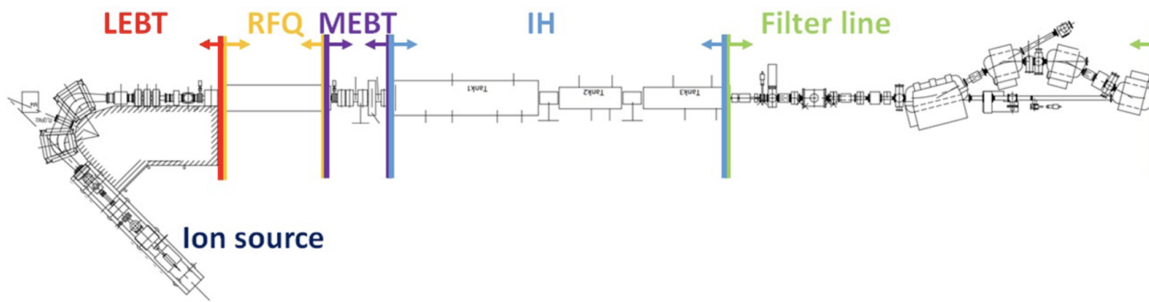


Fig. III.3.11: Linac 3 layout. The ion beam is produced at the source and accelerated in several stages until the filter line where the appropriate charge selection is performed before sending the beam to LEIR through the transfer line.

cooling because it is fast (≤ 0.4 s) at 4.2 MeV/nucleon which are unequalled by other techniques. Finally, the beam is accelerated and extracted to the PS. A detailed description of how multi-turn injection in the transverse and longitudinal phase space is achieved in LEIR can be found in Ref. [1]. The position and the basic shape of LEIR is fixed by the fact that LEIR re-cycles the LEAR (Low-Energy Antiproton Ring) main dipole magnets at their original position. It has almost square geometry, 78.54 m circumference, with four bending sections, each one deflecting the beam by 90° and four straight sections, each one with a total length of about 12.8 m. Figure III.3.12 shows the LEIR machine. Table III.3.6 compiles the most important beam parameters.

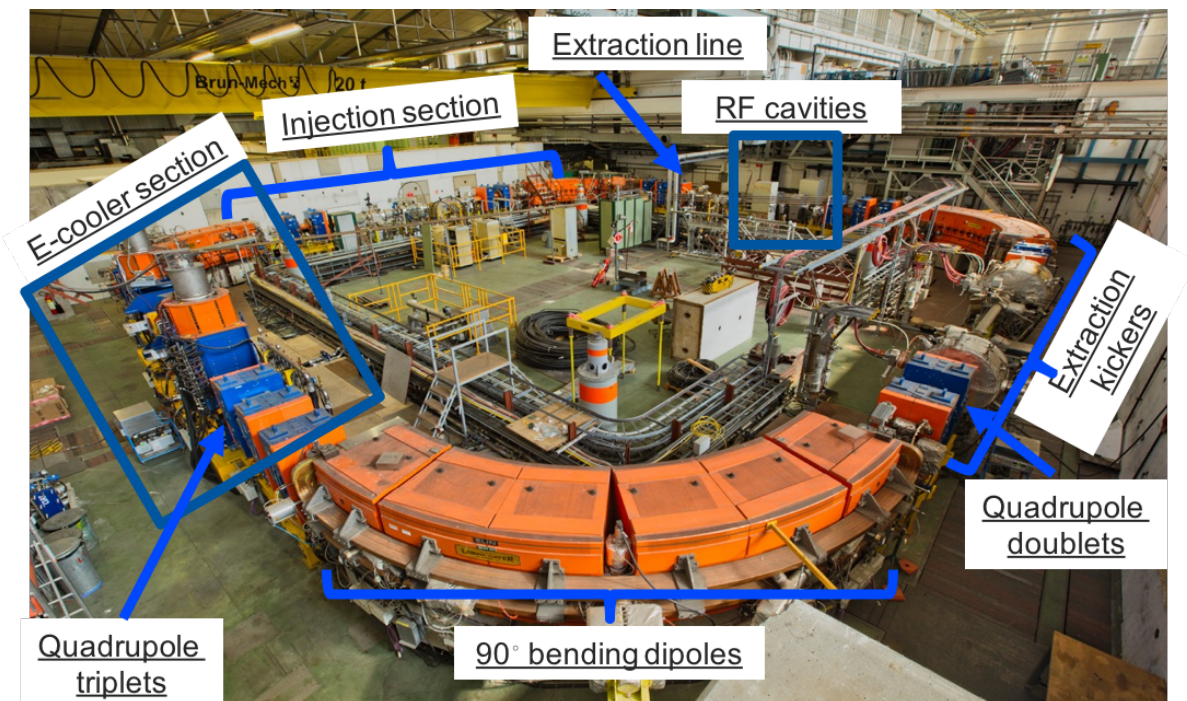


Fig. III.3.12: LEIR layout.

The main LEIR cycle is called NOMINAL and consists of 7 injections of Linac 3 pulses. Due to the high accumulated intensity, electron cooling during this cycle is crucial. Figure III.3.13 shows

Table III.3.6: LEIR beam parameters. The kinetic energy (K) at injection is fixed by the Linac 3 machine. At extraction the LEIR $B\rho$ is fixed to 4.8 Tm, which corresponds to 72.2 MeV/nucleon for Pb^{54+} . The relativistic β and γ , as well as the revolution frequency are given for Pb^{54+} .

	Injection	Extraction
R (m)	12.5	
K (MeV/n)	4.2	72.2
β	0.094	0.37
γ	1.005	1.07
$Q_{x,y}$	1.82, 2.72	
$Q'_{x,y}$	-2.19, -3.74	
γ_{tr}	2.87	
η	-0.87	
α_c	0.1241	
f_{rev}	360 kHz	1.42 MHz
$\epsilon_{n,H,V}$ (mm mrad)	~ 0.4 (after cooling)	
$4\sigma_{t,rms}$ (ns)	800 (h=2)	

the different parts of the NOMINAL cycle and the evolution of the total beam intensity. The beam is captured in two bunches separated by 200 ns, accelerated and extracted. The duration of the cycle is 3.6 s and it is used to prepare the beam for LHC ion physics.

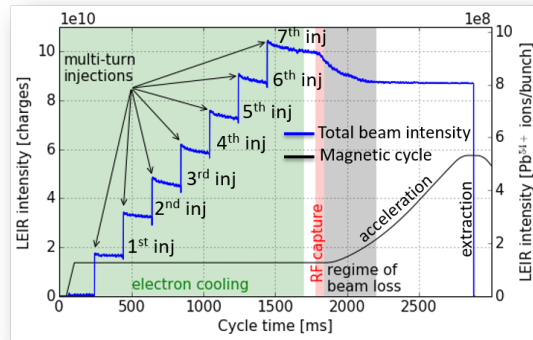


Fig. III.3.13: LEIR NOMINAL cycle.

Since 2015 the LEIR performance has been boosted in order to meet the HL-LHC requirements in terms of bunch intensity and emittance at extraction, i.e. $8.1 \cdot 10^8$ ions per bunch. As can be seen in Fig. III.3.14, which summarises the increase in extracted intensity since 2015, the target has been surpassed since 2016.

III.3.2.4 SPS slip-stacking beams

The upgrade of the RF and LLRF SPS systems during LS2 aimed at implementing momentum slip-stacking for the LHC ion beams to reduce the bunch spacing from 100 to 50 ns and thus to increase the total beam intensity for the HL-LHC project by increasing the number of bunches from 640 pre-LS2 to

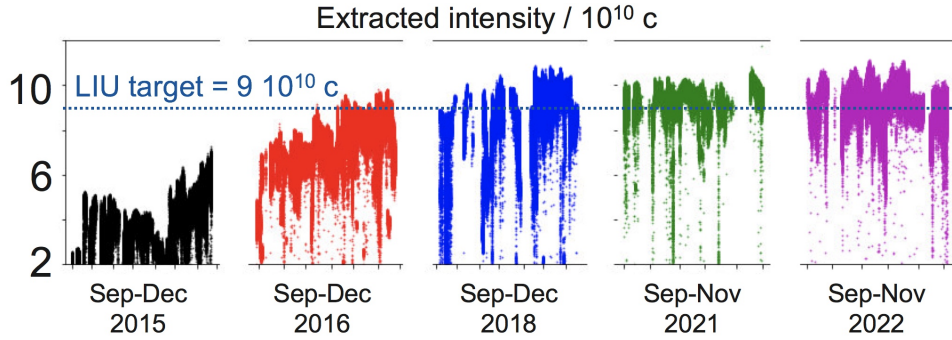


Fig. III.3.14: Evolution of the LEIR extracted lead intensity in number of charges for 2015, 2016, 2018, 2021 and 2022 (2017 is not shown because that year the complex operated xenon).

1240 bunches per beam, and therefore, the instantaneous luminosity to $7 \cdot 10^{27} \text{ cm}^{-2} \text{ s}^{-1}$. Momentum slip-stacking allows two high-energy particle beams of different momenta to slip azimuthally, relative to each other, in the same beam pipe. The two beams are captured by two RF systems with a small frequency difference between them. Each beam is synchronized with one RF system and it is perturbed by the other. The moment the two beams are stacked one on top of the other, the full beam is recaptured with a much higher RF voltage at the average RF frequency, allowing to have 50 ns bunch spacing at the end of the process. The very first LHC ion run with slip-stacking beams took place in 2023. Figure III.3.16 shows the SPS slip-stacking cycle with 14 injections from PS each of 4 bunches. At the end of the injection process the beam is accelerated to 300 GeV where the slip-stacking process takes place. Once finished, the beam made of 56 bunches separated by 50 ns, is accelerated to 450 GeV and extracted to the LHC.

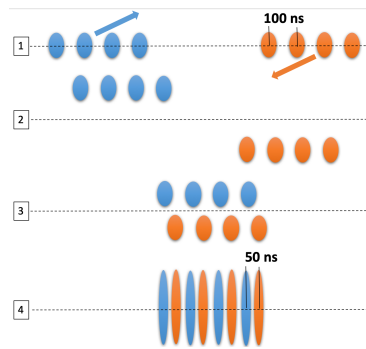


Fig. III.3.15: SPS slip-stacking procedure: PS batches of four bunches each separated 100 ns, of different momenta and different RF frequencies slip longitudinally relative to each other in the same beam pipe. The black line marks $\delta E = E - E_0 = 0$, where E_0 is the design energy. When the two beams are in the correct longitudinal position, the full beam is recaptured with a non-adiabatic voltage jump at the average RF frequency. The resulting bunch spacing is 50 ns.

III.3.2.5 The Large Hadron Collider

The Large Hadron Collider, LHC, is the world-largest and most powerful particle collider. It can collide protons and ions at the maximum beam energy of $7 \cdot Z$ TeV, where Z is the atomic number of the colliding nucleus ($Z=1$ for protons, $Z=82$ for fully stripped lead ions, etc). We refer the reader to Chapter III.4.2, where the main concepts and performance goals of LHC are reviewed, together with the main technical

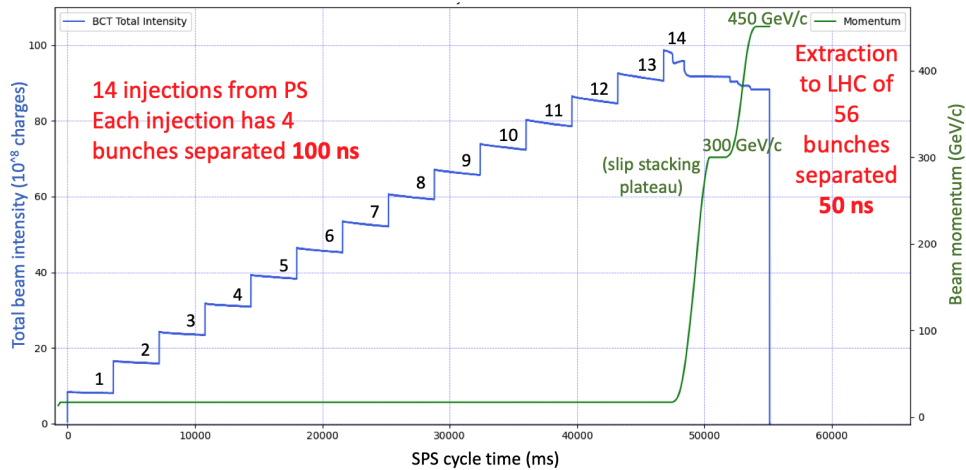


Fig. III.3.16: SPS slip-stacking cycle in 2023 used to fill LHC with HL-LHC ion beam.

challenges and key technological choices.

III.3.3 Experimental areas

The CERN physics programme is very broad, ranging from nuclear to high-energy physics, from studies of antimatter to the possible effects of cosmic rays on clouds. Although the synchrotrons described above are called LHC injectors, they all have their own experimental areas serving a scientific community of several thousand physicists conducting very different experiments. In the following a summary of this rich physics programme is given.

III.3.3.1 Booster experimental areas: ISOLDE

In the transfer line from Booster to PS, radioactive isotopes can be produced via proton-induced target fragmentation, spallation and fission reactions at ISOLDE. ISOLDE was first served by the Synchrocyclotron from 1967 to 1990. Afterwards the Booster took over. ISOLDE is CERN's longest-running experimental site. It uses the 1.4 GeV protons from Booster sent to solid and liquid target materials to produce a wide spectrum of radioactive isotopes up to $A = 92$. The high intensity and large scope of produced isotopes meant that ISOLDE had become a major international facility to perform experiments on radioactive isotopes. At the end of the nineties it was proposed to post accelerate the beams from ISOLDE. The REX ISOLDE accelerator was built and started its operation in 2001.

A major upgrade program, HIE-ISOLDE, was approved in 2009. It represents the next generation of nuclear physics and uses superconducting radiofrequency cavities for accelerating the radioactive beams up to 10 MeV/nucleon with masses up to 200.

The layout of the ISOLDE facility with the different ranges of isotope energies and masses can be found in Fig. III.3.17. The research carried out in ISOLDE not only covers nuclear and atomic physics, but also, astrophysics, fundamental interactions, solid state and life sciences.

Last but not least, a wide range of radioisotopes, some of which can be produced only at CERN thanks to the unique ISOLDE facility, are produced for MEDICIS (Medical Isotopes Collected from ISOLDE). MEDICIS devises and tests unconventional radioisotopes with a view to developing new

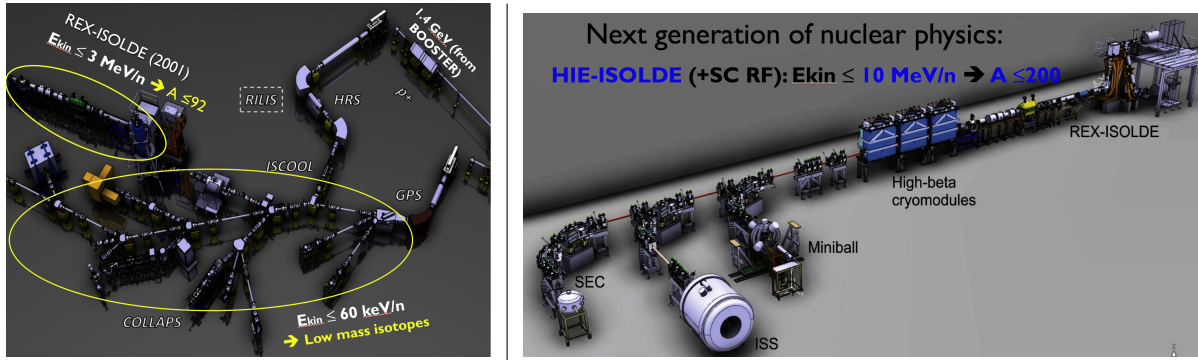


Fig. III.3.17: Left: view of the ISOLDE and REX-ISOLDE; right: view of HIE-ISOLDE.

approaches to fight cancer for hospitals and research centres in Switzerland and across Europe.

III.3.3.2 PS experimental areas: EAST AREA, n_TOF

The 26 GeV proton beam from PS is sent to a target placed in the EAST AREA (EA), see Fig. III.3.18, to create secondary beams of electrons, hadrons and muons with momentum ranging from 1 to 15 GeV/c and up to $2 \cdot 10^6$ particles per spill. The ions from LEIR are also sent to EA. The secondary beams are used for detector calibration, proton, neutron and ion irradiation in IRRAD, CHARM and the future CHIMERA/HEARTS facilities, and for climate research. Indeed, a study of the influence of galactic cosmic rays on the Earth’s climate through the media of aerosols and clouds, is carried out in CLOUD (Cosmics Leaving Outdoor Droplets), that began operation in November 2009.

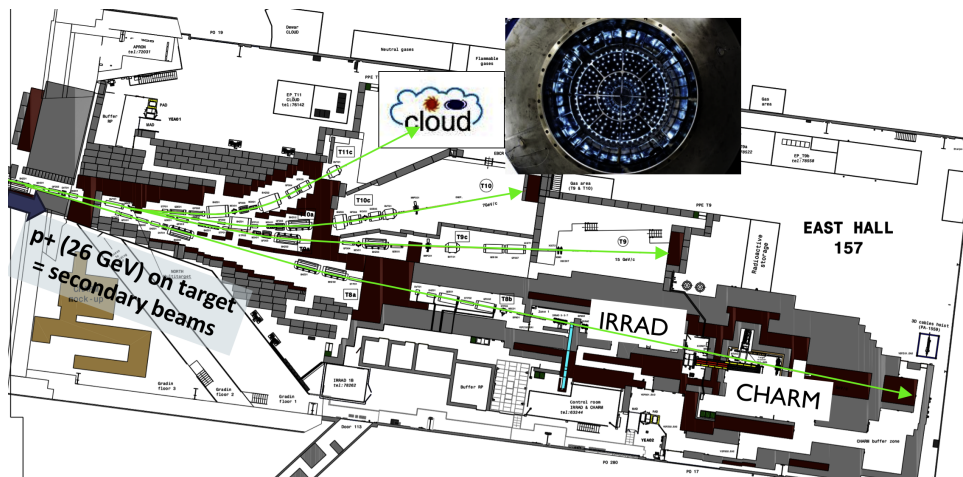


Fig. III.3.18: PS East Area layout.

The study of neutron-induced reactions is of large importance in a wide variety of research fields, ranging from stellar nucleosynthesis, symmetry breaking effects in compound nuclei, and the investigation of nuclear level densities, to applications of nuclear technology, including the transmutation of nuclear waste, accelerator-driven systems and nuclear fuel cycle investigations. This crucial area of research is carried out at CERN by the n_TOF facility. The PS protons extracted at 20 GeV/c are sent towards a lead spallation target to produce neutrons. Each primary proton produces around 300 neutrons

with energies ranging from meV to GeV. The neutron kinetic energy is determined by the time-of-flight technique along a 185 m long tube instrumented at the end with a Total Absorption Calorimeter, see Fig. III.3.19, performing high-quality neutron capture measurements of small mass and/or radioactive samples.

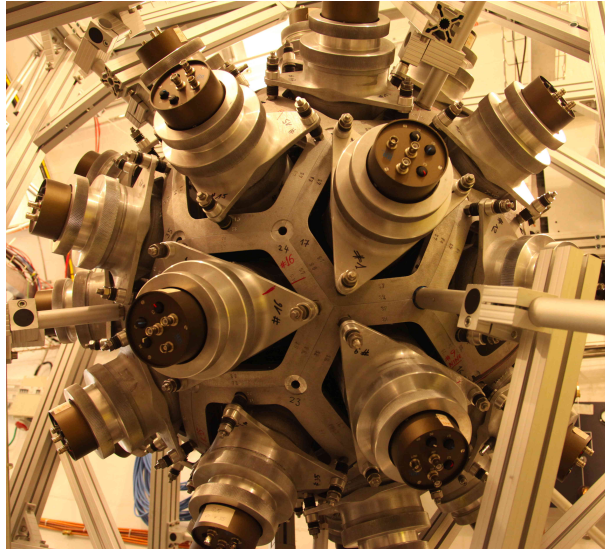


Fig. III.3.19: View of the n_TOF Total Absorption Calorimeter.

III.3.3.3 SPS experimental areas: North Area, HiRadMat, AWAKE

Similar to the PS EA, the SPS North Area (NA) is a facility where the up to 400 GeV/c proton beams and the up to 150 GeV/nucleon ion beams are used for fixed-target experiments. There are seven beam lines, totalling 5.8 km. A sketch of the SPS NA can be seen in Fig. III.3.20. There are four target stations and six beam lines distributed in three experimental halls, EHN1, EHN2 and ECN3. It has permanent experiments like NA61/SHINE, a quark-gluon plasma experiment that performs complementary searches to ALICE, in the H2 beam line; the NA64-e experiment in the H4 beam line that performs a competitive dark-photon search with high purity electron beams; the NA62 experiment in ECN3 to search for very rare kaon decays; the NA58/COMPASS experiment in EHN2 to study hadron structure and hadron spectroscopy with hadron and muon beams. It also has beam lines for detector calibration and irradiation, in particular for the LHC detectors and for detectors that will be placed in satellites and in the International Space Station.

The SPS also serves the first proton-driven Plasma Wake Acceleration (PWA) experiment worldwide, the AWAKE experiment, where a 400 GeV/c proton beam with $3 \cdot 10^{11}$ protons per bunch is sent into a 10 m long rubidium plasma chamber to create a wake-field. Once the wake created, a 10 to 20 MeV electron beam is sent into the plasma and accelerated by the plasma wake up to 2 GeV. This unique concept was demonstrated in 2018. While classical RF cavities can accelerate up to 10 MeV per meter, PWA can reach up to 500 GeV per meter. The AWAKE layout can be seen in Fig. III.3.21.

Current and future accelerators operate with higher energy, higher intensity, smaller size beams. For example, LHC nominal beams with 2808 bunches with $1.5 \cdot 10^{11}$ protons per bunch at 7 TeV, have

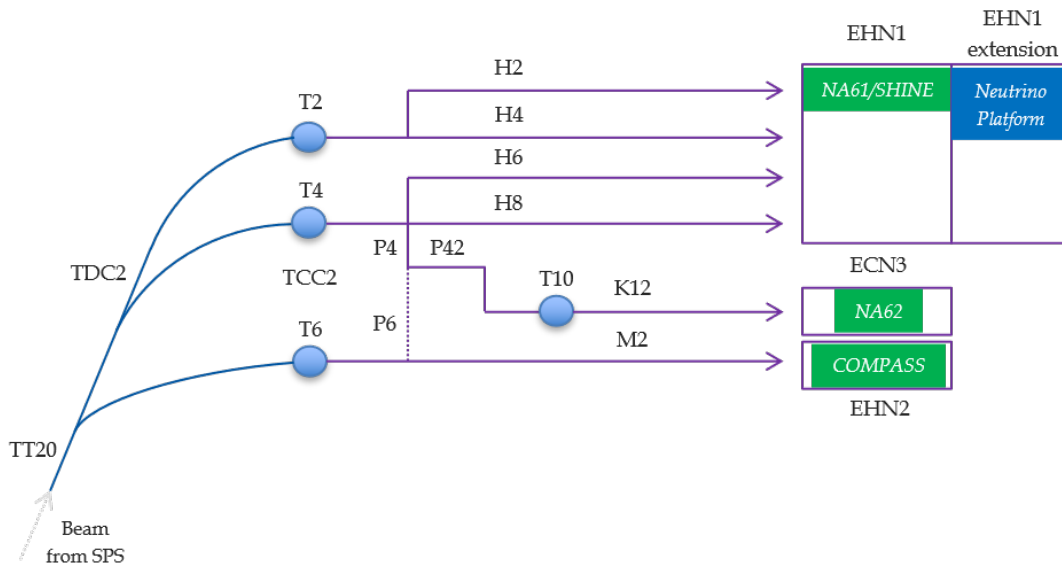


Fig. III.3.20: Scheme of the SPS North Area.

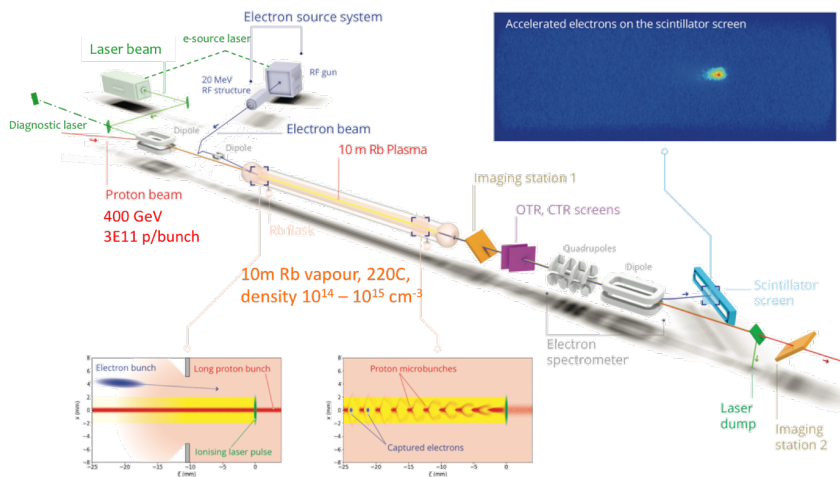


Fig. III.3.21: Scheme of the AWAKE experiment.

a stored energy of 362 MJ per beam, which can melt 500 kg of cooper. HiRadMat is a facility designed to study the impact of intense pulsed beams on materials, in particular, thermal management, radiation damage, thermal shock and beam-induced pressure waves. There is no other facility in the world that can produce and study such energetic beams, except in the LHC itself. Therefore, such an experimental line was needed to be able to advance in new material technology development.

III.3.4 Antiproton Decelerator (AD) and ELENA

Last but not least, at CERN the first anti-atoms were created in laboratory conditions in 1995 at CERN's Low Energy Antiproton Ring (LEAR) facility, that later on became LEIR. Nine of these atoms were produced in collisions between antiprotons and xenon atoms over a period of 3 weeks. Each one remained in existence for about 40 billionths of a second, travelled at nearly the speed of light over a path of 10

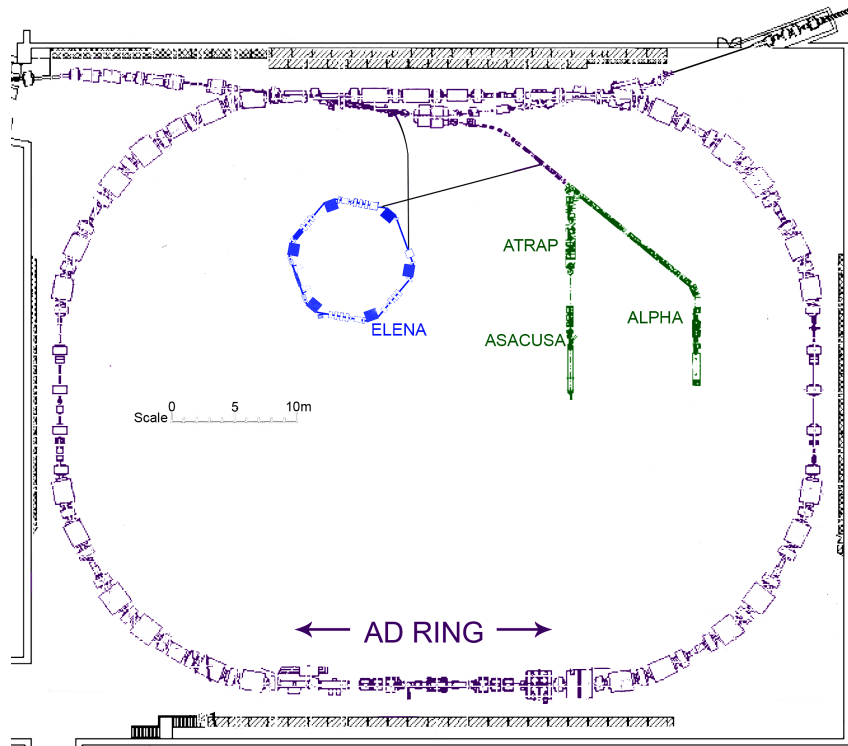


Fig. III.3.22: Layout of the AD and ELENA synchrotrons.

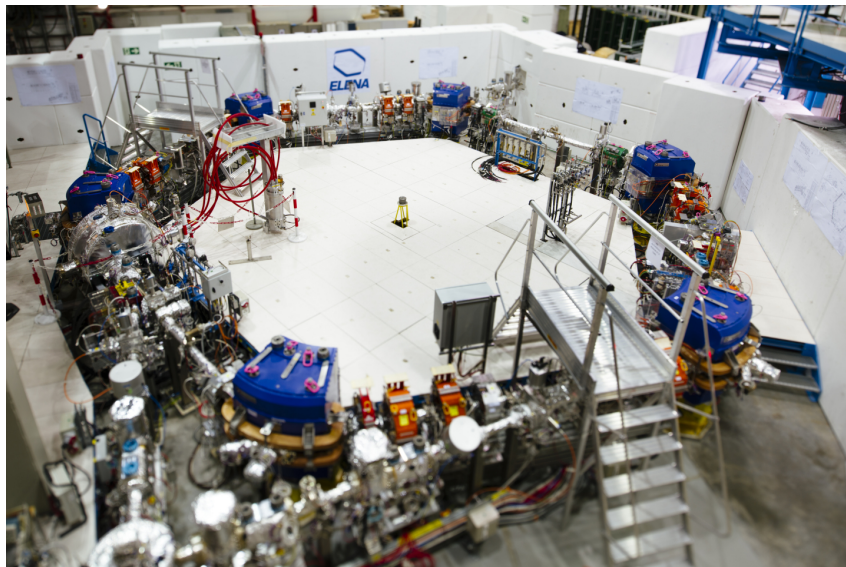


Fig. III.3.23: View of ELENA ring.

metres and then annihilated with ordinary matter. This was the first step in a programme to make detailed measurements of antihydrogen. The programme continued in 1997 when the Antiproton Decelerator (AD) was approved and built in 1999. The 26 GeV/c protons from PS are sent to an iridium target to produce 1 antiproton every 10^7 proton collisions. The antiprotons are focused and captured in the AD and decelerated to 100 MeV/c, i.e. from the speed of light down to 10% of the speed of light, keeping the emittance under control with a mixture of electron and stochastic cooling. All this process takes about

one minute. The 200 m circumference AD synchrotron sends the beam to ELENA, the Extra Low Energy Antiproton Ring, a 30 m circumference post decelerator, commissioned in 2020, that decreases the beam momentum down to 13.7 MeV/c, which corresponds to a kinetic energy of 100 keV. Figure III.3.22 shows the layout of the two synchrotrons and the experimental lines towards ATRAP, ASACUSA and ALPHA experiments. Figure III.3.23 shows a picture of the machine as installed.

Since the Antimatter Decelerator Complex entered operation many milestones have been reached in the pursuit of matter-antimatter differences. In 2002 ATHENA and ATRAP created thousands of atoms of antimatter in a “cold” state, i.e. slow-moving atoms that can be studied before they annihilate with ordinary matter. In 2011 ALPHA trapped antimatter atoms for over 16 minutes: long enough to begin to study their properties in detail. The same year, ASACUSA experiment at CERN reported a new measurement of the antiproton’s mass accurate to about one part in a billion. One of the latest publications by ALPHA, in September 2023, reports about the observation of the effect of gravity on the motion of antimatter. ALPHA shows that antihydrogen atoms behave in a way consistent with gravitational attraction to the Earth. Repulsive ‘antigravity’ is, therefore, ruled out in this case. This experiment paves the way for precision studies of the magnitude of the gravitational acceleration between anti-atoms and the Earth to test the weak equivalent principle of general relativity.

References

- [1] M. Benedikt *et al.* (Eds.), LHC design report, v. 3, CERN-2004-003-V-3 (CERN, Geneva, 2004), [doi:10.5170/CERN-2004-003-V-3](https://doi.org/10.5170/CERN-2004-003-V-3).
- [2] F. Gerigk and M. Vretenar (Eds.), Linac4 technical design report, CERN-2020-006 (2006), [doi:10.23731/CYRM-2020-006](https://doi.org/10.23731/CYRM-2020-006).
- [3] J. Coupard *et al.* (Eds.), LHC injectors upgrade, CERN-ACC-2014-0337 (2014), [doi:10.17181/CERN.7NHR.6HGC](https://doi.org/10.17181/CERN.7NHR.6HGC).
- [4] J. Coupard *et al.* (Eds.), LHC injectors upgrade, CERN-ACC-2016-0041 (2016), [doi:10.17181/CERN.L6VM.UOMS](https://doi.org/10.17181/CERN.L6VM.UOMS).
- [5] D.J. Warner (Ed.), CERN Heavy Ion Facility Design Report, CERN-93-01 (1993), [doi:10.5170/CERN-1993-001](https://doi.org/10.5170/CERN-1993-001).
- [6] D.J. Warner, The Heavy Ion Linac for the CERN Lead Ion Facility, in Proc. 17th International Linac Conference, Tsukuba, Japan, 21–26 Aug. 1994, Eds. K. Nakahara, K. Takata, and Y. Yamazaki, (KEK, Tsukuba, 1995), pp. 654–658, [doi:10.17181/CERN-PS-94-34-HI](https://doi.org/10.17181/CERN-PS-94-34-HI).
- [7] H.D. Haseroth, The CERN Heavy Ion Facility, CERN-PS-94-27-HI (CERN, Geneva, 1994), [doi:10.17181/CERN-PS-94-27-HI](https://doi.org/10.17181/CERN-PS-94-27-HI).
- [8] P. Lefèvre and T. Pettersson, The Large Hadron Collider: Conceptual design, CERN-AC-95-05-LHC (CERN, Geneva, 1995), [doi:10.17181/CERN-AC-95-05-LHC](https://doi.org/10.17181/CERN-AC-95-05-LHC).
- [9] D. Brant, Review of the LHC ion programme, LHC-Project-Report-450 (CERN, Geneva, 2000), [doi:10.17181/LHC-Project-Report-450](https://doi.org/10.17181/LHC-Project-Report-450).
- [10] P. Lefèvre and D. Möhl, Lead ion accumulation scheme for LHC, in Workshop on Beam Cooling and Related Topics, Montreux, Switzerland, 4–8 Oct. 1993, Ed. J. Bosser (CERN, Geneva, 1994), [doi:10.5170/CERN-1994-003.411](https://doi.org/10.5170/CERN-1994-003.411).

- [11] P. Lefèvre and D. Möhl, A low energy accumulation ring of ions for LHC (A feasibility study), CERN-PS-93-62-DI, LHC Note 259 (CERN, Geneva, 1993), [doi:10.17181/CERN-PS-93-62-DI](https://doi.org/10.17181/CERN-PS-93-62-DI).
- [12] M. Chanel, LEIR: The Low Energy Ion Ring at CERN, *Nucl. Instrum. Methods Phys. Res. A* **532** (2004) 137–143, [doi:10.1016/j.nima.2004.06.040](https://doi.org/10.1016/j.nima.2004.06.040).
- [13] I. Béjar Alonso (Ed.), High-Luminosity Large Hadron Collider (HL-LHC): Technical design report, CERN-2020-010 (CERN, Geneva, 2020), [doi:10.23731/CYRM-2020-0010](https://doi.org/10.23731/CYRM-2020-0010).
- [14] R. Geller, *Electron cyclotron resonance ion sources and ECR plasmas* (Routledge, New York, NY, 1996), [doi:10.1201/9780203758663](https://doi.org/10.1201/9780203758663).
- [15] C.E. Hill *et al.*, Experience with the GTS-LHC ion source, in *3rd LHC Project Workshop: 15th Chamonix Workshop Chamonix, Divonne-les-Bains, Switzerland, 23–27 Jan. 2006*, Ed. J. Poole (CERN, Geneva, 2006), pp. 240–242, [doi:10.17181/CERN.SU34.XA3D](https://doi.org/10.17181/CERN.SU34.XA3D).